第 35 卷第 8 期 无 机 化 学 学 报 Vol.35 No.8
2019 年 8 月 CHINESE JOURNAL OF INORGANIC CHEMISTRY 1485-1492

用于超级电容器的层状 Co_3O_4/Ti 纳米片柔性电极及其低电荷转移电阻

韩丹丹*,[1] 赵 远[1] 申 烨[1] 丁元生[1] 程振玉[1] 景晓燕*,[2] 张学仪*,[3]
([1]吉林化工学院化学与制药工程学院,吉林 132022)
([2]哈尔滨工程大学材料科学与化学工程学院,哈尔滨 150001)
([3]吉林中西医结合医院,吉林 132012)

摘要:采用水热合成法,在 Ti 网上原位生长多孔层状 Co_3O_4 纳米片,并优化了电荷转移电阻。通过 X 射线衍射(XRD)、扫描电子显微镜(SEM)和透射电子显微镜(TEM)对产物的结构、形貌进行表征,及对电极的电化学性能进行测试。结果表明,材料是由排列良好的微米矩形二维薄片组成,且具有均匀的孔隙分布。这种独特的微纳米结构的超级电容器电极材料降低了电极的电荷转移电阻,增强了活性物质的结构稳定性,从而提高了电极的电化学性能,在电流密度为 100 mA·g^{-1} 时,电极循环 1 000 次后,电容保持率为 91.8%,电荷转移电阻(R_{ct})为 0.29 Ω。这些显著的超电容性能归因于合理的二维层状结构在柔性基底钛网上的生长及柔性 Co_3O_4/Ti 电极活性材料的高利用率。

关键词:柔性电极;层状 Co_3O_4;多孔纳米片;转移电阻;超级电容器
中图分类号:O646 **文献标识码**:A **文章编号**:1001-4861(2019)08-1485-08
DOI:10.11862/CJIC.2019.165

Layered Co_3O_4/Ti Nanosheet Flexible Electrode with Low Transfer Resistance for Supercapacitor

HAN Dan-Dan*,[1] ZHAO Yuan[1] SHEN Ye[1] DING Yuan-Sheng[1]
CHENG Zhen-Yu[1] JING Xiao-Yan*,[2] ZHANG Xue-Yi*,[3]
([1]*College of Chemistry and Pharmaceutical Engineering, Jilin Institute of Chemical Technology, Jilin, Jilin* 132022, *China*)
([2]*College of Materials Science and Chemical Engineering, Harbin Engineering University, Harbin* 150001, *China*)
([3]*Jilin Hospital of Integrated Traditional Chinese and Western Medicine, Jilin, Jilin* 132012, *China*)

Abstract: The layered Co_3O_4 nanosheets with porous nature on Ti mesh were adopted to optimize the transfer resistance by a facile hydrothermal method. The synthesized materials were characterized using X-ray diffraction (XRD), scanning electron microscopy (SEM), transmission electron microscopy (TEM) and electrochemical techniques. The results showed that the materials consisted of well-arranged micrometer length rectangular 2D flakes with uniform pore distribution. This unique microstructure obtained the electrode lower transfer resistance, higher structure stability, and better electrochemical performance for supercapacitor. The 2D porous layered Co_3O_4 nanosheet could achieve a relatively good capacitance retention of 91.8% at a current density of 100 mA·g^{-1} after 1 000 cycles and a low transfer resistance (R_{ct}) of 0.29 Ω. These remarkable supercapacitive performances are attributed to the rationally 2D layered structure on flexible Ti mesh substrate, high utilization ratio of active materials of the flexible Co_3O_4/Ti electrode.

Keywords: flexible electrode; layered Co_3O_4; porous nanosheets; transfer resistance; supercapacior

收稿日期:2019-03-28。收修改稿日期:2019-05-17。
国家自然科学基金(No.21401073)、吉林省科技厅自然科学基金(No.20170101211JC)和吉林化工学院重大科技项目(No.2018019)资助。
*通信联系人。E-mail:luckhan2006@163.com

0 Introduction

The urgent demand for wearable electronic devices has attracted increasing interests in flexible and lightweight energy storage devices[1-2]. Supercapacitors emerge from other candidates because of the high power density, charge/discharge rate and efficient cycle stability[3-4]. In accordance with the energy storage mechanisms, supercapacitors can be divided into electrochemical double-layer capacitors (EDLCs) which store energy physically at the electrodes surface within electrolyte and pseudocapacitors which store energies by fast redox reactions[5-7]. Conventional supercapacitors are usually based on activated carbon electrodes which have high power density, long cycle life, and rapid charging/discharging rate[8]. However, among the series of pseudocapacitors electrode materials for supercapacitor applications, transition metal oxides are widely studied due to variable oxidation states of metal ions which facilitate redox transitions and higher charge storage within the potential range of water decomposition[9-10]. Generally, the metal oxides with the following characteristics could be a super candidate as supercapacitor electrode materials[11-16]: (1) Metal may coexist in two or more oxidation states without phase transition in a continuous range and without modification of an irreversible three-dimensional structure; (2) The transition metal oxide should be electronically conductive; (3) The protons can be freely released and inserted into the oxidation lattice during the redox. Co_3O_4 is considered to be one of the better alternate materials because of their rich oxidation states, low cost, high theoretical specific capacitances, and environment friendly nature. Since charge storage is directly related to surface properties, controlling the surface morphology of electrode materials has a great influence on their electrochemical properties. Although various structures have been demonstrated to be quite feasible for high performance and stable electrodes, the design of the layered structure plays a more critical role for high performance supercapacitor applications, because layered structures can be flake-off resistant and better tolerant to high rate redox reactions[17-21].

As a method to improve the conventional process, the *in situ* growth of active materials on a flexible substrate has attracted extensive attention, because they can be used as the finished electrode directly[22-23]. As expected, this method improves the performance of the electrodes. Some progress has been made in foam, fiber and paper substrate. The general method of fabricating 3D arrays structures involves chemical preparation of Co_3O_4 and assembly of various architectures[24-26]. These processes, however, always bring in some defects and impurities resulting in poor conductivity.

Based on the survey above, a convenient and scalable hydrothermal based approach to deposit layered Co_3O_4 nanosheets directly grown on flexible titanium mesh substrate as a binder-free electrode for low ion-transfer resistance has been designed. The layered Co_3O_4 was composed of uniform rectangular and micrometer length 2D flakes. These highly layered Co_3O_4 materials with nanostructures were functioned directly as supercapacitors electrodes without further treatment delivered lower ion-transfer resistance and good cycle stability.

1 Experimental

1.1 Synthesis procedure

All reagents were purchased from the Aladdin Chemical Reagent Company and were used without further purification. Generally, 2.5 mmol $Co(NO_3)_2$ and 12.5 mmol $CO(NH_2)_2$ were dissolved in 30 mL distilled water with constant stirring to obtain a settled solution. Then, the pre-treated titanium mesh (1 cm×1 cm) and the settled solution were transferred into a Teflon-lined stainless steel autoclave. The stainless steel autoclave was maintained at 95 ℃ for 8 h, and then cooled to room temperature. Finally, the samples were treated at 350 ℃ for about 3.5 h.

1.2 Characterizations

The crystalline information of the as-prepared products was analyzed by X-ray diffraction (XRD, DX-2700 Dandong Haoyuan, Cu $K\alpha$, λ=0.154 05 nm, operating voltage=40 V, operating current=30 mA, the

scan rate =0.33° ·s^{-1}, 2θ =30° ~85°). The structural investigation of the layered Co_3O_4 samples were determined using a scanning electron microscope (SEM, JSM-6480A, Japan Electronics, operating voltage=20 V) and high-resolution transmission electron microscopy (HRTEM, FEI, Tecnai G^2 F20, 120 kV).

1.3 Electrochemical measurements

The electrochemical tests were performed by a three-electrode system with a 2.0 mol·L^{-1} KOH electrolyte. Pt foils and a saturated calomel electrode (SCE) were used as the counter electrode and the reference electrode. The loaded weight of the active materials was controlled to be approximately 3.1 mg·cm^{-2}.

The specific capacitance (C_s) of the Co_3O_4 sample was calculated from the cyclic voltammetry (CV) curves according to Equation (**1**)[10,27]:

$$C_s=(\int IdV)/(vmV) \quad (1)$$

where I is the current (A), m is the mass of active material (g), v and dV are the potential scan rate and the differential of potential.

The C_s was also calculated by discharge curves[28-29]:

$$C_s=I\Delta t/(m\Delta V) \quad (2)$$

Where I is applied current density (A), m is the mass of the sample (g), Δt is discharge time (s), and ΔV is operating potential (V).

2 Results and discussion

2.1 Structural investigation

Fig.1 illustrates the fabrication procedure of the layered Co_3O_4 nanosheets on Ti mesh. Firstly, urea broken down into HCO_3^-, and then the major precursor of $Co_2(OH)_2CO_3$ were prepared by the reaction of Co^{2+} with CO_3^{2-} and OH^- in the mixed solution. The purple precursor on Ti mesh appeared after the reactions and rinsed with distilled water several times. After calcinations at 350 ℃ for 3.5 h, layered Co_3O_4 electrode was obtained. The advantage of the integrative Co_3O_4 directly grown on flexible substrate is that it can avoid the traditional volume loss caused by the process of mixing active materials with conductive additives and polymer binder[30-31].

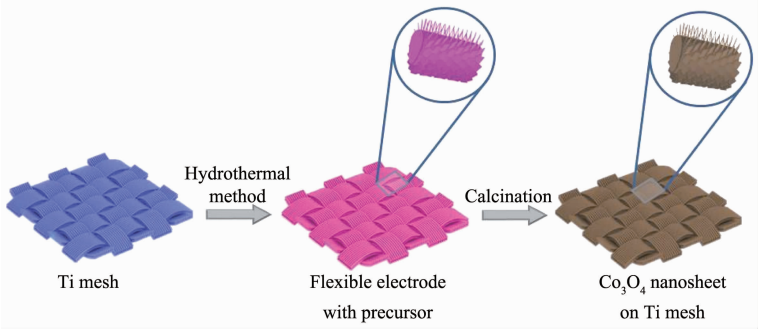

Fig.1　Typical fabrication process of flexible layered Co_3O_4 nanosheet electrodes

The XRD pattern of the layered Co_3O_4 nanosheets on Ti mesh is shown in Fig.2. Except for some diffraction peaks originating from Ti mesh, the well-defined peaks of The peak of Co_3O_4 nanosheet at 31.3°, 36.9°, 44.8°, 59.4°, 65.2° and 82.6° could be indexed to (220), (311), (400), (511), (440) and (444) plane of the layered Co_3O_4 crystalline, respectively, which is in accord with the standard XRD pattern of cubic Co_3O_4 (PDF No.42-1467). No other crystalline phases could be detected, suggesting that the high purity of the obtained Co_3O_4 nanosheet.

The morphologies of the layered Co_3O_4 nanosheets

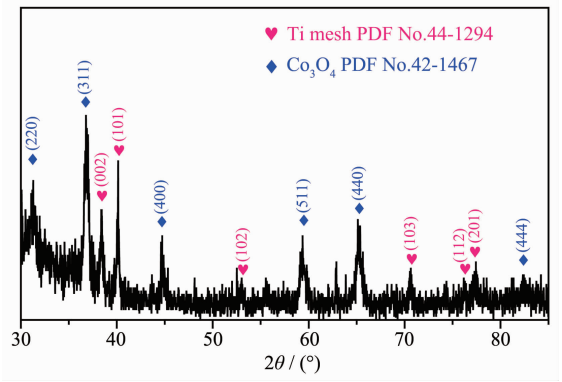

Fig.2　XRD pattern of the layered Co_3O_4 nanosheet array on Ti mesh

on Ti mesh were investigated by SEM. It was clear that Co precursor could be grown uniformly at large scale on skeletons of Ti mesh (Fig.3). The sample showed the layered morphology with well-arranged 2D microsheets. A detailed observation revealed that the bunches of Co_3O_4 were vertically and regularly distributed but leaving a highly open interspace which endowed fast transport of the electrolyte. These nanosheets had an edge length of 2~3 μm and a uniform thickness of less than 20 nm.

The detailed structure of the single Co_3O_4 nanosheets was further investigated by TEM, as shown in Fig.4. It can be seen that Co_3O_4 nanosheet possessed the abundant pores on its surface, which could be attributed to the gas ejection during the themal transformation from precusor to Co_3O_4 nanosheets. The nanosheet was composed of numerous interconnected nanoparticles with diameters of 5~10 nm, and showed

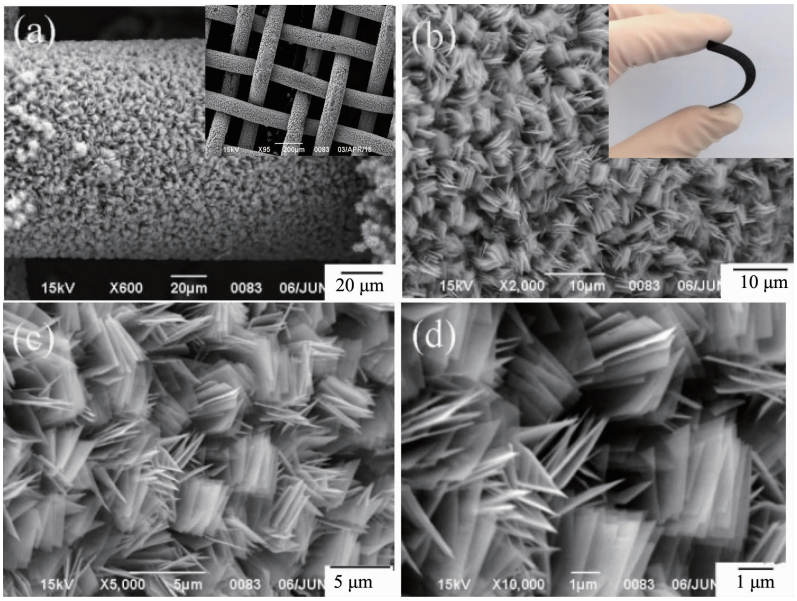

Inset of (a) and (b) were the low resolution SEM images of Co_3O_4 and the Ti mesh substrate respectively

Fig.3 (a, b) Low and (c, d) high magnification SEM images of Co_3O_4 sample

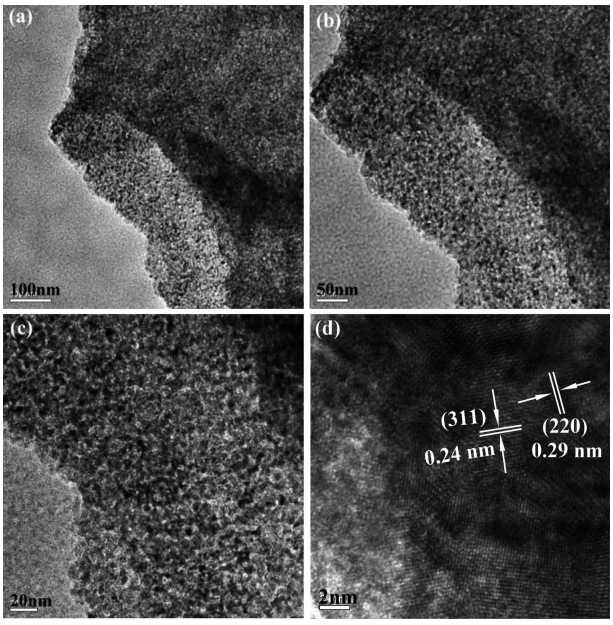

Fig.4 (a, b) Low-magnification TEM images of the mesoporous Co_3O_4 nanosheet; (c,d) HRTEM images of the edge part of the Co_3O_4 nanosheet

a mesoporous structure with a pore size of 2~5 nm. Accordingly, the electrolyte can easily pass in and out of the porous structure and transfer between the layers, forming a shorter diffusion path. The high-resolution TEM (HRTEM) image in Fig.4d revealed the inter-planar spacing of ~0.24 and ~0.29 nm, corresponding to the (311) and (220) plane of Co_3O_4 given in the standard files. Moreover, the SEM images further proved the flexible nature of the Ti mesh substrate, as shown in Fig.3(b).

2.2 Electrochemical measurements

In order to evaluate the electrochemical characteristics of the layered Co_3O_4 samples, the electrochemical measurements were carried out using a three-electrode system in a 2 mol·L^{-1} KOH solution.

Fig.5a shows the CV curves of the layered Co_3O_4 electrode at different scan rates of 5~100 mV·s^{-1}. One pair of redox peaks at various scan rates was clearly observed. Well-fined redox peaks were clearly displayed in all the curves, suggesting the capacitive characteristics of Faradic redox reaction in the electrodes. The possible redox reactions might be described as follows[32]:

$$Co_3O_4+OH^-+H_2O \rightleftharpoons 3CoOOH+e^- \quad (3)$$

$$CoOOH+OH^- \rightleftharpoons CoO_2+H_2O+e^- \quad (4)$$

The C_s at different scan rates in the CV measurements were calculated using the Equation (**1**) (Fig.5b). At scan rates of 5~100 mV·s^{-1}, the C_s for layered Co_3O_4 samples are found to be 64~49 F·g^{-1}. The higher C_s and ~25% capacitance loss when the scan rate increased from 5 to 100 mV·s^{-1} attributee to the larger electroactive surface area of the layered morphology and easy accessibility of OH^- ions for highly feasible redox reactions. Galvanostatic constant current charge-discharge curves at various current densities at the electrochemical window of 0~0.45 V are shown in Fig.5c. The linear slopes and presence of triangular symmetry with respect to the charging/

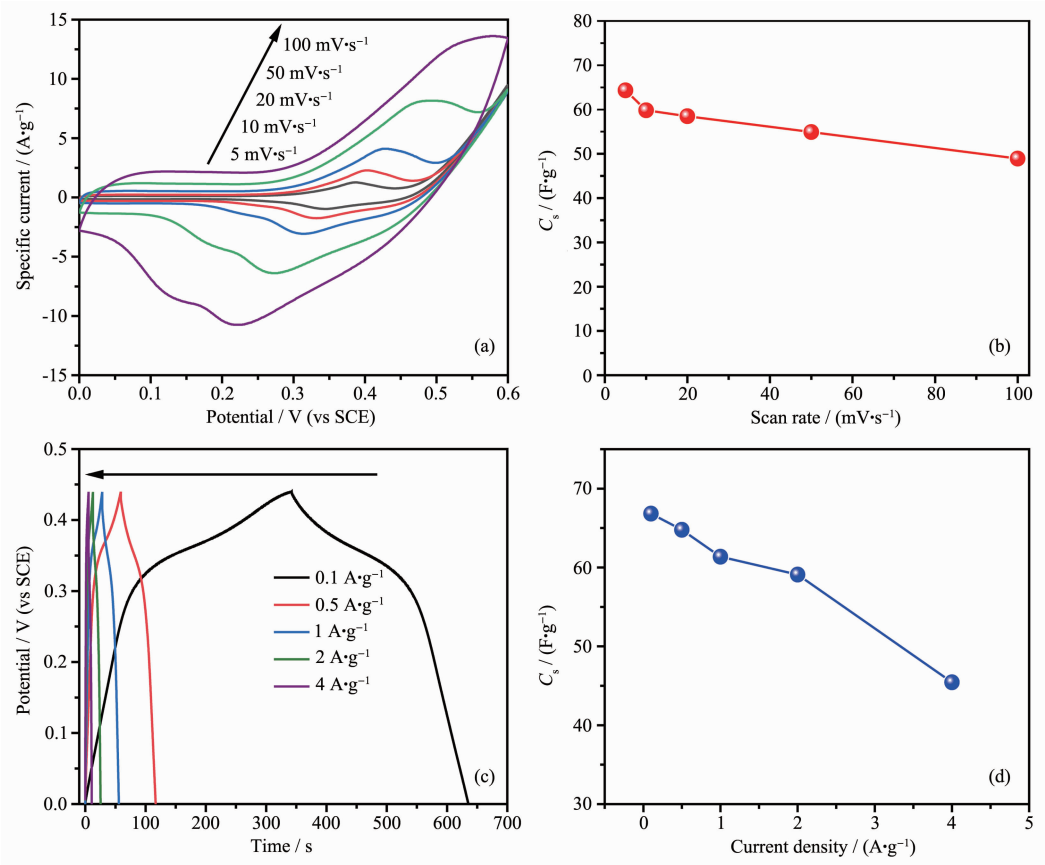

Fig.5 (a) CV curves of layered Co_3O_4 nanosheet electrode at different scan rates; (b) C_s as a function of scan rate; (c) Charge and discharge curves of samples at different current densities; (d) C_s as function of discharge current densities of layered Co_3O_4 electrode

discharging curves confirmed a good electrochemical performance. At a current density of 0.1 $A \cdot g^{-1}$, C_s of Co_3O_4 sample was 67 $F \cdot g^{-1}$, and found that the C_s decreased with increasing current density. The decrease in C_s at high current densities was due to an increase in the internal diffusion resistance within the pseudoactive material, which decreased the efficiency of utilization of the active material.

To further evaluate the electrochemical behavior of the electrode material, electrochemical impedance spectroscopy (EIS) was also collected with a frequecy ranging from 100 kHz to 0.1 Hz at open circuit potential, and the corresponding Nyquist plots are exhibited in Fig.6. The inset in Fig.6 was the equivalent circuit fitted by ZSimpWin. The EIS data can be fitted by internal resistance (R_s), charge transfer resistance (R_{ct}), double layer capacitor (C_{dl}), Warburg impendence (Z_w), and C_{ps} for the limited pseudo-faradic reaction, as shown in the inset in Fig.6. In the high frequency region, the spectra of layered Co_3O_4 electrode showed a semicircle, and the intercept of arc on the x-axis was represented the R_s with a value of 3.09 Ω, which included intrinsic resistance of ionic resistance of electrolyte, and contact resistance with current collector. The R_{ct} related to the semicircle was estimated as 0.29 Ω, which demonstrated much lower resistance to many other Co_3O_4 electrode reported before (Table 1)[19,33-40]. The high-rate capability and excellent reversibility were attributed to the following reasons [41-42]: (1) layered structures can be resisted structural collapse and spalling, which better tolerant to high rate redox reactions during the electrochemical process; (2) layered morphology provided favourable long-range, uniform, stable and smooth oxide conductivity paths; (3) proper porosity of the material is beneficial to the penetration of electrolyte, thus reducing charge transfer resistance.

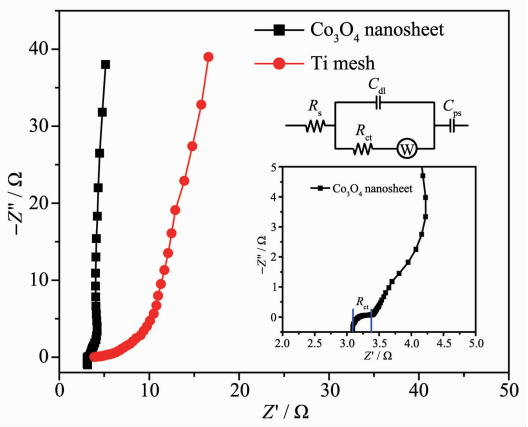

Fig.6 Nyquist plots of layered Co_3O_4 nanosheet and Ti mesh

The cycle life is another important factor for evaluating the performance of supercapacitor. The cyclic performance of layered Co_3O_4 sample for 1 000 cycles at current density of 100 $mA \cdot g^{-1}$ is presented in Fig.7.

During the 1 000 charge-discharge processes, the corresponding coulombic efficiency approached 98%, which confirmed that the material possesseed good reversibility. A capacitance retention of 91.8% was observed after 1 000 charge-discharge cycles, indicating the excellent stability of the 2D porous layered nanosheets electrode.

Table 1 R_{ct} for different structured metal oxide

Electrode	Electrolyte	R_{ct} / Ω	Reference
Layered Co_3O_4 nanosheet	KOH (2 $mol \cdot L^{-1}$)	0.29	This work
Ultrathin Co_3O_4 nanosheets	KOH (6 $mol \cdot L^{-1}$)	≈0.3	[33]
Ultrathin Co_3O_4 nanomeshes	KOH (2 $mol \cdot L^{-1}$)	≈3	[19]
Co_3O_4/graphene	KOH/polyvinyl alcohol	20.66	[34]
Co_3O_4 nanosheet	KOH (2 $mol \cdot L^{-1}$)	0.06	[35]
Co_3O_4@carbon nanotube	KOH (0.5 $mol \cdot L^{-1}$)	≈2.5	[36]
NiO nanosheet arrays	KOH (1 $mol \cdot L^{-1}$)	0.66	[37]
ZnO/Co_3O_4 nanorod	KOH (1 $mol \cdot L^{-1}$)	87.9	[38]
Co_3O_4@MnO_2 nanosheet	KOH (1 $mol \cdot L^{-1}$)	≈50	[39]
Tremella-like NiO@Co_3O_4@MnO_2	KOH (6 $mol \cdot L^{-1}$)	≈1	[40]

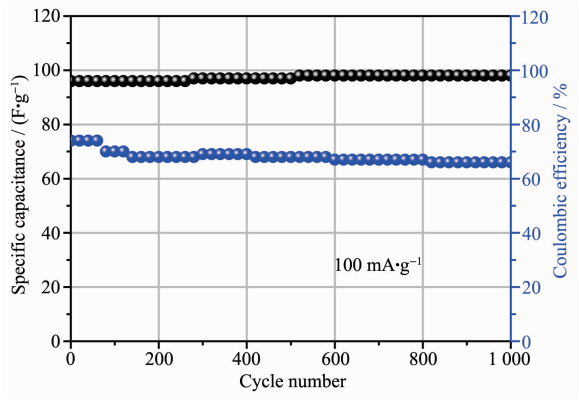

Fig.7　Long cycle performance of Co_3O_4 nanosheet arrays measured at the current density of 100 mA·g^{-1}

3　Conclusions

In summary, layered Co_3O_4 on Ti mesh have been synthesized by a facile route as flexible supercapacitor electrode. The prepared layered Co_3O_4 nanosheets possessed long-range 2D conductivity paths with high surface area and porous nature, which exhibited excellent electrochemical performance towards the EIS, such as lower charge transfer resistance (R_{ct}). This layered Co_3O_4 with the excellent structural and electrochemical stability with 98% coulombic effeciency may be very useful for the flexible electrode for the energy storage devices.

References:

[1] Guo D, Luo Y Z, Yu X Z, et al. *Nano Energy*, **2014**,**8**:174-182

[2] Nishide H, Oyaizu K. *Science*, **2008**,**319**:737-738

[3] Simon P, Gogotsi Y. *Nat. Mater.*, **2008**,**7**:845-854

[4] Wang G P, Zhang L, Zhang J J. *Chem. Soc. Rev.*, **2012**,**41**:797-828

[5] Chen L F, Huang Z H, Liang H W, et al. *Adv. Funct. Mater.*, **2014**,**24**:5104-5111

[6] Ling M, Qian X Y, Zhu D Z, et al. *Chin. Chem. Lett.*, **2019**, https://doi.org/10.1016/j.cclet.2019.03.010.

[7] Kumbhar V S, Kim D H. *Electrochim. Acta*, **2018**,**271**:284-296

[8] Xue D F, Zhu D Z, Xiong W, et al. *ACS Sustainable Chem. Eng.*, **2019**,**7**:7024-7034

[9] Hu Q Q, Gu Z X, Zheng X T, et al. *Chem. Eng. J.*, **2016**,**304**:223-231

[10]Zhang Z Y, Liu S S, Xiao F, et al. *ACS Sustainable Chem. Eng.*, **2017**,**5**:529-536

[11]Jiang J, Liu J P, Huang X T, et al. *Cryst. Growth Des.*, **2010**,**10**:70-75

[12]Qiu K, Lu Y, Cheng J, et al. *Electrochim. Acta*, **2015**,**157**:62-68

[13]Wang X H, Yao S W, Wu X X, et al. *RSC Adv.*, **2015**,**5**:17938-17944

[14]Liu T, Zhang L Y, You W, et al. *Small*, **2018**,**14**:1702407

[15]Li Z P, Yu X Y, Paik U. *J. Power Sources*, **2016**,**310**:41-46

[16]Qorbani M, Naseri N, Moshfegh A Z. *ACS Appl. Mater. Interfaces*, **2015**,**7**:11172-11179

[17]Meher S K, Rao G R. *J. Phys. Chem. C*, **2011**,**115**:15646-15654

[18]Xu Y Q, Wang Z L, Tan L, et al. *Ind. Eng. Chem. Res.*, **2018**,**57**:5259-5267

[19]Wei G J, Zhou Z, Zhao X X, et al. *ACS Appl. Mater. Interfaces*, **2018**,**10**:23721-23730

[20]Chen D H, Peng L L, Yuan Y F, et al. *Nano Lett.*, **2017**,**17**:3907-3913

[21]Sennu P, Aravindan V, Lee Y S. *J. Power Sources*, **2016**,**306**:248-257

[22]Wang Y, Huang J, Xiao Y J, et al. *Carbon*, **2019**,**147**:146-153

[23]Yu L Y, Hu L F, Anasori B, et al. *ACS Energy Lett.*, **2018**,**3**:1597-1603

[24]Aloqaylia S, Ranaweeraa C K, Wanga Z, et al. *Energy Storage Mater.*, **2017**,**8**:68-76

[25]Xu R, Lin J M, Wu J H, et al. *Appl. Surf. Sci.*, **2018**,**434**:861-870

[26]An K L, Zheng Y, Xu X X, et al. *J. Solid State Chem.*, **2019**,**270**:539-546

[27]Shakir D, Shahid M, Rana U A, et al. *Electrochim. Acta*, **2014**,**129**:28-32

[28]Saray M T, Hosseini H. *Electrochim. Acta*, **2016**,**222**:505-517

[29]Chen C, Zhou J J, Li Y L, et al. *J. Solid State Chem.*, **2019**,**271**:239-245

[30]Luo G X, Teh K S, Xia Y, et al. *J. Alloys Compd.*, **2018**,**767**:1126-1132

[31]Feng C, Zhang J F, He Y, et al. *ACS Nano*, **2015**,**9**:1730-1739

[32]Pan G X, Xia X H, Cao F, et al. *Electrochim. Acta*, **2015**,**173**:385-392

[33]Xiao Z Y, Fan L L, Xu B, et al. *ACS Appl. Mater. Interfaces*, **2017**,**9**:41827-41836

[34]Liao Q Y, Li N, Jin S X, et al. *ACS Nano*, **2015**,**9**:5310-5317

[35]Rakhi R B, Chen W, Hedhili M N, et al. *ACS Appl. Mater. Interfaces*, 2014,6:4196-4206

[36]Wang X W, Li M X, Chang Z, et al. *ACS Appl. Mater. Interfaces*, **2015**,**7**:2280-2285

[37]Huang M, Li F, Ji J Y, et al. *CrystEngComm*, **2014**,**14**:2878-2884

[38]Gao M, Wang W K, Rong Q, et al. *ACS Appl. Mater. Interfaces*, **2018**,**10**:23163-23173

[39]Guo W, Hou L L, Hou B, et al. *J. Alloys Compd.*, **2017**,**708**:524-530

[40]Wang H, Ren Q, Brett D J L, et al. *J. Power Sources*, **2017**, **343**:76-82

[41]Wu X, Han Z C, Zheng X, et al. *Nano Energy*, **2017**,**31**:410-417

[42]Ouyang Y, Huang R J, Xia X F, et al. *Chem. Eng. J.*, **2019**, **355**:416-427